No model to rule them all: a systematic comparison of 83 thermal performance curve models across traits and taxonomic groups

Dimitrios - Georgios Kontopoulos[1,2,3,✉], Arnaud Sentis[4], Martin Daufresne[4], Anthony I. Dell[5,6], & Samraat Pawar[1]

[1]Department of Life Sciences, Imperial College London, Silwood Park, Ascot, Berkshire, SL5 7PY, UK

[2]LOEWE Centre for Translational Biodiversity Genomics, Senckenberganlage 25, 60325, Frankfurt, Germany

[3]Senckenberg Research Institute, Senckenberganlage 25, 60325, Frankfurt, Germany

[4]INRAE, Aix Marseille University, UMR RECOVER, 3275 Route de Cézanne - CS 40061, 13182 Aix-en-Provence Cedex 5, France

[5]National Great Rivers Research and Education Center, One Confluence Way, 62024, East Alton, Illinois, USA

[6]Department of Biology, Washington University in St. Louis, 1 Brookings Drive, 63130, St. Louis, Missouri, USA

✉email: dgkontopoulos@gmail.com

Abstract

In ectotherms, the performance of physiological, ecological, and life-history traits universally increases with temperature to a maximum before decreasing again. Identifying the most appropriate thermal performance model for a specific trait type has broad applications, from metabolic modelling at the cellular level to forecasting the effects of climate change on population, ecosystem, and disease transmission dynamics. To date, numerous mathematical models have been designed, but a thorough comparison among them is lacking. In particular, we do not know if certain models consistently outperform others, and how factors such as sampling resolution and trait or organismal identity influence model performance. These have led researchers to select models semi-arbitrarily, potentially introducing biases that compromise environmental suitability predictions. To fill these gaps, we collect 2,739 thermal performance datasets from diverse traits and taxa, to which we fit 83 models used in previous studies. We detect remarkable variation in model performance which is not primarily driven by sampling resolution, trait type, or taxonomic information. Our results highlight a lack of well-defined scenarios in which certain models are more appropriate than others. Therefore, to avoid likely model-specific biases, future studies should perform model selection to identify the most appropriate model(s) for their data.

Introduction

All physiological, ecological, and life-history traits of ectotherms, from metabolic rates to population growth rates and species interactions, are strongly influenced by temperature. The relationship between trait performance and temperature is known as the "thermal performance curve" (TPC) or the "thermal reaction norm" (Fig. 1A) and is unimodal and usually asymmetric[1,2]. Determining the most appropriate TPC model for a given trait dataset, and how the shape of the TPC varies across trait types, taxonomic groups, and environments have a wide range of applications across biological systems and levels of organisation, from cellular metabolic modelling[3–5] and ontogenetic growth[6–8], to population[9–11], community[12–14], ecosystem[15–17], and disease dynamics[18–20]. TPCs have also recently become integral to predicting the effects of climatic warming as well as thermal fluctuations on biological systems[21–24].

A wide variety of TPC models have been developed since the first two (one symmetric and one asymmetric) were proposed by Janisch back in 1925[27]. TPC models span the spectrum of phenomenological (e.g., based on a modification of the Gaussian distribution[28,29]) to mechanistic (based on biochemical kinetics[30–34]) mathematical equations. Many of the phenomenological models were initially developed for specific traits or species groups (e.g., for the development rate of arthropods[35–37]).

This smorgasbord of TPC models begs the question of whether certain models are more appropriate than others for specific trait datasets. For example, it is commonly assumed that fundamental physiological traits (e.g., respiration, photosynthesis) should be best-fitted by mechanistic models derived from biochemical kinetics principles[30–34,38,39]. This is because the parameters of such models can (in theory) describe the underlying enzyme reaction that determines the shape of the TPC. In contrast, higher-order traits that cannot be linked to the activity of a single rate-limiting enzyme (e.g., overall dynamic body acceleration, resource

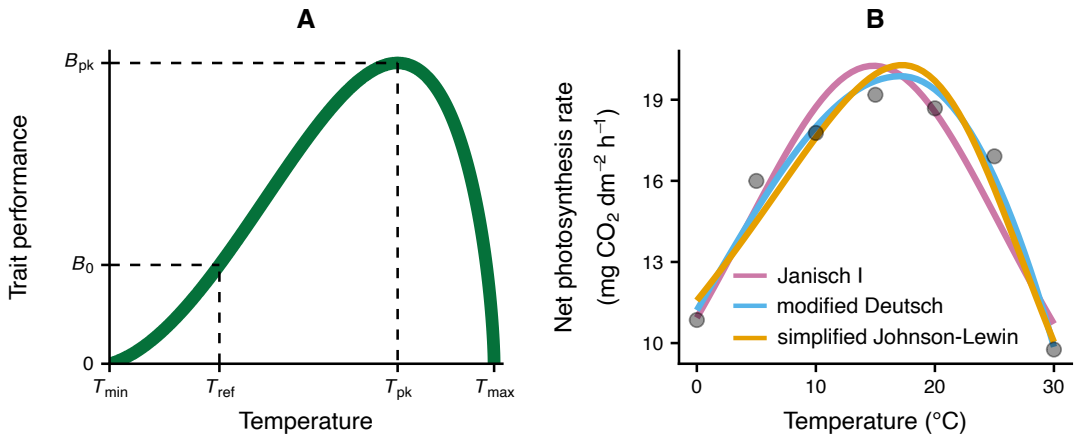

Fig. 1: The thermal performance curve (TPC) illustrates the influence of temperature on the performance of a biological trait of an individual ectotherm, a population, or even a whole ecosystem. TPCs can be estimated by fitting a wide range of nonlinear mathematical models to trait measurements obtained at multiple temperatures. Some parameters commonly included in such models are explicitly shown in panel A. T_{min} and T_{max} are the temperatures above and below which trait values are positive. T_{pk} is the temperature at which the TPC reaches its maximum height (B_{pk}). B_0 is the performance at a reference temperature (T_{ref}) below T_{pk}, often quantified for comparison of baseline performance across TPCs from different individuals or species[25]. Panel B shows three different models (see Supplementary section S5) fitted to net photosynthesis rate measurements of *Erigeron annuus*[26]. Note that the resulting TPCs differ in their T_{pk} and B_{pk} values, as well as in their degree of skewness, with the TPC of the Janisch I model being fully symmetric.

consumption) are expected to be best described by phenomenological models, whose parameters reflect various aspects of TPC shape (e.g., where the T_{min}, T_{pk}, and T_{max} lie; see Fig. 1A). Another assumption is that for high resolution datasets (with numerous experimental temperatures), parameter-rich models will systematically outperform simple alternatives, e.g., revealing two different slopes at the rising part of the TPC[40–42]. Such fine-scale variation in TPC shape is assumed to be generally present but hard to detect because most thermal performance datasets tend to be small[43].

Whether such assumptions are valid has yet to be objectively and systematically determined, with all previous such studies being limited in their scope in terms of the number and types of models compared, types of traits, and of diversity of taxonomic groups[28,44–49]. Even in recent studies that introduce new general models (expected to apply well to any dataset)[32–34,50], a thorough performance comparison between the new model and other pre-existing ones is typically missing. As a result, in studies quantifying the temperature dependence of experimental trait data, TPC models are typically chosen (semi-)arbitrarily and with little justification. This practice could occasionally worsen the signal-to-noise ratio of a dataset or, at worst, introduce model-specific biases that could be hard to control for[48] (see Fig. 1B). For example, consider a trait with a roughly symmetric TPC, such as per capita fecundity[51]. For this trait, models that force the fall of the TPC to be steeper than its rise will necessarily yield misleading estimates of the slopes before and after the thermal optimum. Furthermore, some datasets may not have adequate statistical power for objectively estimating all the parameters of a complex and parameter-rich model ("parameter unidentifiability"), in which case multiple sets of parameter estimates will produce effectively identical curves. One could treat this spurious variation in parameter estimates as real rather than a purely statistical artefact and may attempt to come up with mechanistic explanations for it.

To fill this gap, here we compile an extensive set of TPC models which we fit to multiple datasets of experimental TPCs from the literature. We then compare models on the basis of

i) how well they fit experimental data and of ii) how similar their fits tend to be. By doing so, we address three key questions:

1. Are there models that consistently outperform others across any dataset?
2. For thermal performance datasets with high resolution, do parameter-rich models perform better than simpler ones?
3. Do mechanistic models fit fundamental physiological traits better than phenomenological models?

Results and discussion

Sources of thermal performance datasets

We combined previously published datasets of thermal performance of i) population growth rate of bacteria, archaea, and phytoplankton[52,53], ii) photosynthesis and respiration rate of algae, aquatic, and terrestrial plants[54], iii) metabolic rate of zooplankton[55–57] and other heterotrophic ectotherms[58], iv) development rate of damselflies[59] and helminths[60], v) overall dynamic body acceleration of elasmobranchs[61], and vi) numerous other biological traits included in the Biotraits database[62].

Our data compilation includes 3,598 datasets of thermal performance (i.e., measurements of trait performance vs temperature for a single taxon from a specific location and study), with at least four distinct temperatures per dataset. These were filtered down to 2,739 datasets (see Methods), spanning more than 100 traits from all seven kingdoms[63] and from 39 phyla (Fig. 2).

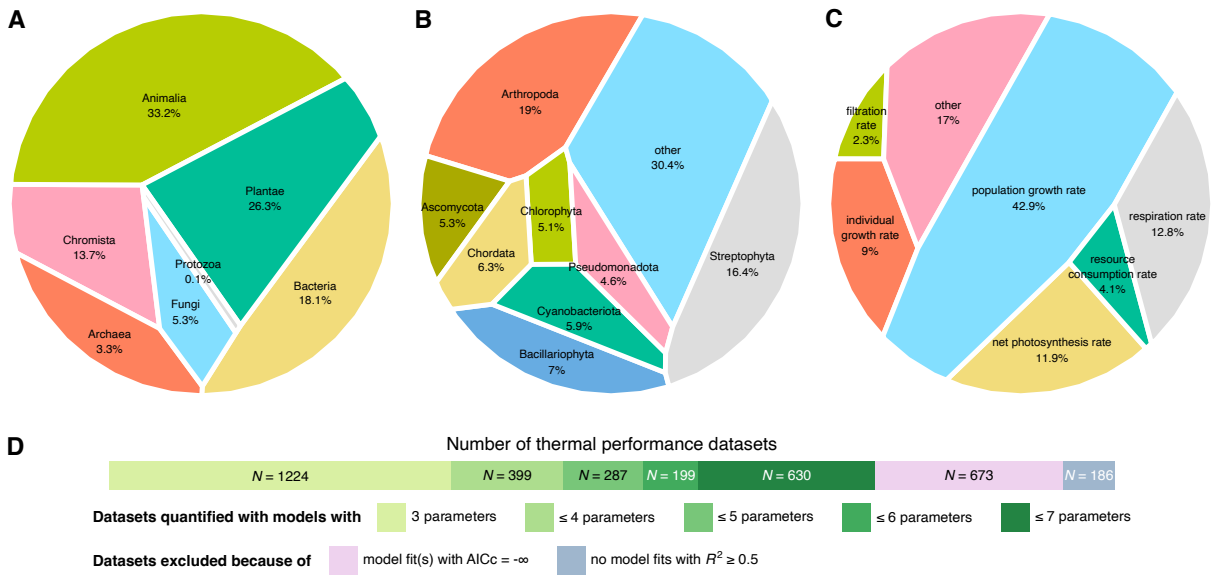

Fig. 2: Characteristics of thermal performance datasets included in this study. Panels A, B, and C show the breakdown of the most common kingdoms, phyla, and traits, respectively, in our data compilation. Panel D shows the number of thermal performance datasets to which various models could be fitted, as well as datasets that were excluded from this study.

Compilation of a TPC model catalogue

To collect published TPC models, we queried Google Scholar using terms such as "thermal performance curve model", "thermal performance curve equation", "thermal reaction norm model", "temperature response curve model" etc. From the resulting hits, we progressively added models that could capture the entire TPC (i.e., not just its rise or fall) and that were not mathematically equivalent to any model that was already in the list. For example, the equation of the Johnson-Lewin model[30,43] is equivalent to that of a particular 4-parameter variant of the Sharpe-Schoolfield model[25,40]. We did not include models that can only be fitted to multiple thermal performance datasets at the same time (e.g., through a hierarchical Bayesian approach[50]) and not to individual datasets. We also ensured that each included model could adequately fit (see next section) at least a single dataset from a

representative subset of our data compilation. This process yielded 83 distinct TPC models (see Supplementary section S5 for their equations, free parameters, and references).

Comparison of model performance across datasets

We fitted the 83 models separately to each thermal performance dataset (see Methods) and, for each fit, we calculated the R^2 and the Akaike Information Criterion value, using the correction for small sample size (AICc[64]). After removing model fits with an R^2 value below 0.5 (see Supplementary Fig. 1 for the distribution of R^2 values of retained fits), we calculated the AICc weight of each model for each thermal performance dataset. We also constructed a matrix of median pairwise Euclidean distances among models, from which we inferred a dendrogram of models (see Methods) to identify those that generally produce very similar fits (Fig. 3).

The first question that we addressed was whether some models systematically outperform others, irrespective of dataset. This was not the case as model performance varied strongly across thermal performance datasets, with no model consistently reaching high AICc weights throughout (Fig. 3). It is worth noting, however, that certain models (e.g., Gaussian, simplified Briere I, second-order polynomial, Mitchell-Angilletta, Eubank) performed relatively well across many datasets.

Fig. 3 (on next page): Comparison of the 83 TPC models across 2,739 thermal performance datasets. Left: dendrogram of models based on the similarity of the fits that they produce. Branch lengths represent median Euclidean distances among resulting TPC fits (see Methods). Models based on biochemical kinetics are shown in pink, whereas phenomenological models are in black. Right: The AICc weight of each model (rows) for each dataset (columns). Note that columns have been ordered so that datasets with similar patterns of AICc weights are within close proximity of each other. The figure was rendered using the `ggtree`[65] (v. 2.2.4) and the `ComplexHeatmap`[66] (v.2.12.1) R packages.

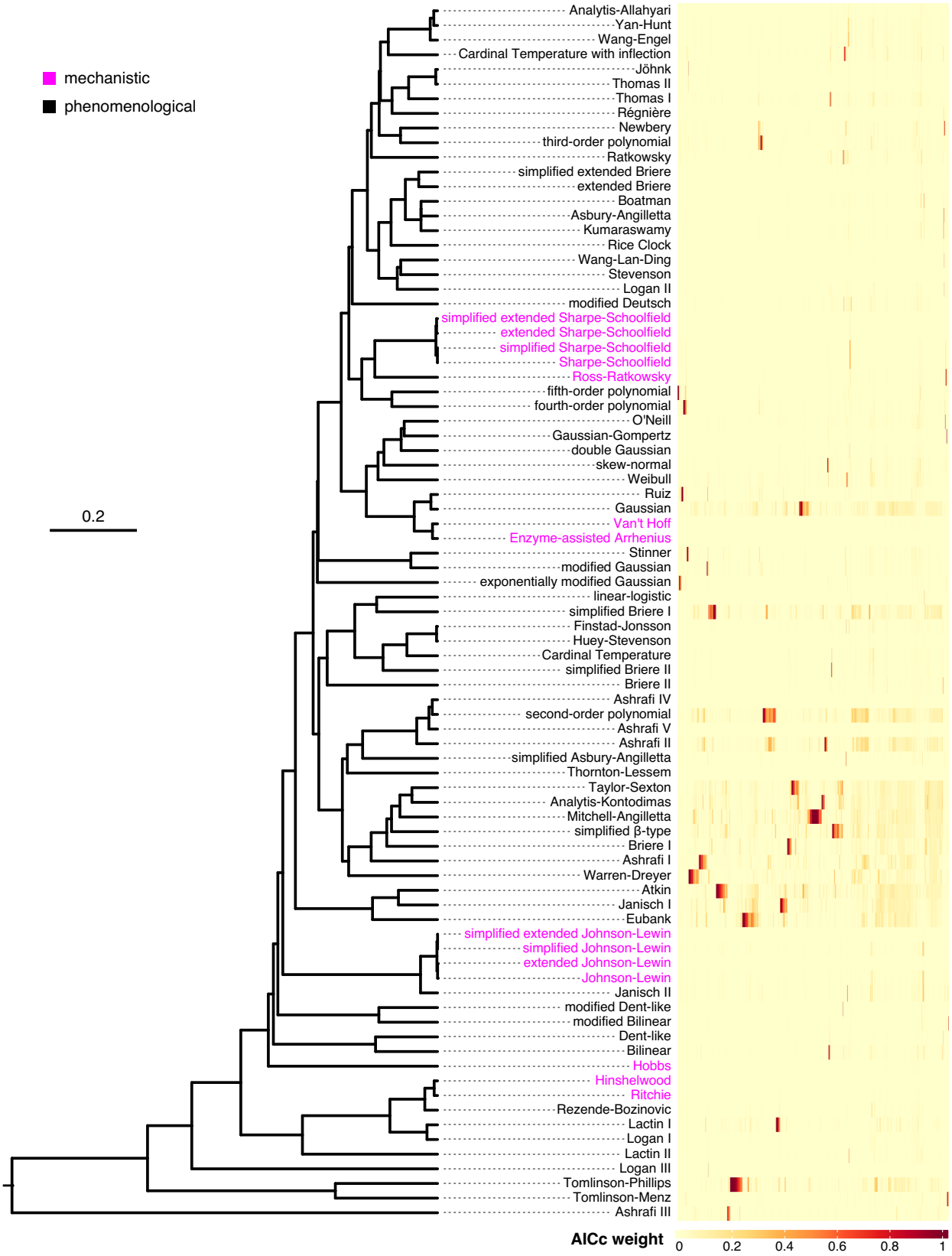
mechanistic
phenomenological
0.2
Analytis-Allahyari
Yan-Hunt
Wang-Engel
Cardinal Temperature with inflection
Jöhnk
Thomas II
Thomas I
Régnière
Newbery
third-order polynomial
Ratkowsky
simplified extended Briere
extended Briere
Boatman
Asbury-Angilletta
Kumaraswamy
Rice Clock
Wang-Lan-Ding
Stevenson
Logan II
modified Deutsch
simplified extended Sharpe-Schoolfield
extended Sharpe-Schoolfield
simplified Sharpe-Schoolfield
Sharpe-Schoolfield
Ross-Ratkowsky
fifth-order polynomial
fourth-order polynomial
O'Neill
Gaussian-Gompertz
double Gaussian
skew-normal
Weibull
Ruiz
Gaussian
Van't Hoff
Enzyme-assisted Arrhenius
Stinner
modified Gaussian
exponentially modified Gaussian
linear-logistic
simplified Briere I
Finstad-Jonsson
Huey-Stevenson
Cardinal Temperature
simplified Briere II
Briere II
Ashrafi IV
second-order polynomial
Ashrafi V
Ashrafi II
simplified Asbury-Angilletta
Thornton-Lessem
Taylor-Sexton
Analytis-Kontodimas
Mitchell-Angilletta
simplified β-type
Briere I
Ashrafi I
Warren-Dreyer
Atkin
Janisch I
Eubank
simplified extended Johnson-Lewin
simplified Johnson-Lewin
extended Johnson-Lewin
Johnson-Lewin
Janisch II
modified Dent-like
modified Bilinear
Dent-like
Bilinear
Hobbs
Hinshelwood
Ritchie
Rezende-Bozinovic
Lactin I
Logan I
Lactin II
Logan III
Tomlinson-Phillips
Tomlinson-Menz
Ashrafi III
AICc weight
0
0.2
0.4
0.6
0.8
1

To understand if complex models increasingly outperform simpler alternatives as the number of experimental temperatures increases, we next identified the ten models with the highest median AICc weights across datasets with i) 4, ii) 5-7, or iii) 8 or more distinct temperatures. Even for the highest resolution group, the ten models with the highest average performance had either three or four parameters (Fig. 4C). Moreover, datasets of low, moderate, and high resolution shared five three-parameter models among their top ten. It is worth pointing out that the top ten models in the three resolution groups had median AICc weights that were not higher than 0.05 and interquartile ranges that often included values that were effectively zero (Fig. 4).

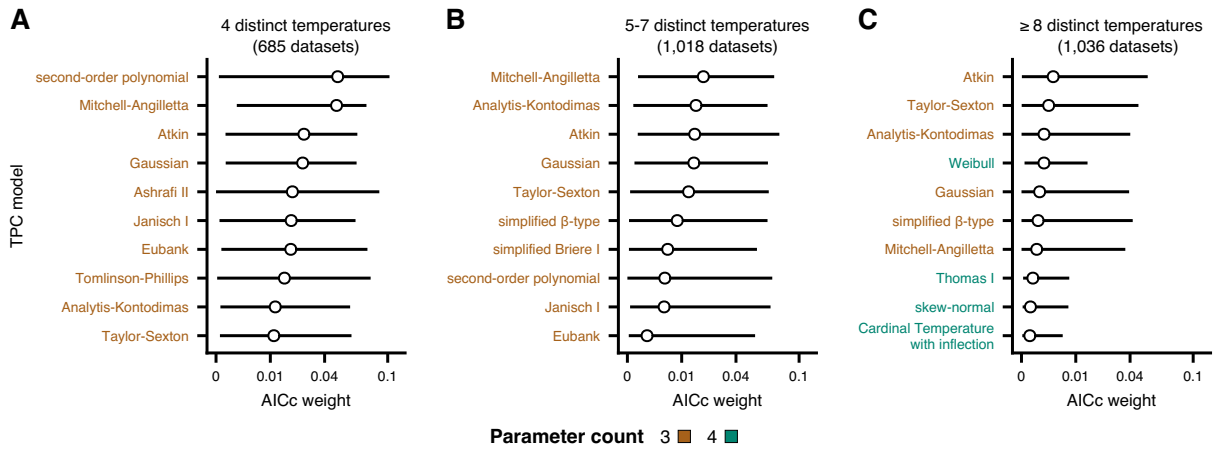

Fig. 4: The ten best-fitting models across datasets of low (A), moderate (B), or high resolution (C). Circles represent the median AICc weight, whereas horizontal bars stand for the interquartile range. Model performance varies remarkably within each panel, whereas five three-parameter models are among the top ten in all three panels. Even for datasets with 8 or more distinct temperatures, the best-performing models have only three (brown) or four parameters (green). Note that values along the horizontal axes do not increase linearly.

Our third and final question was to determine if mechanistic models (whose parameters describe the activity of underlying rate-limiting enzymes) exhibit better performance than phenomenological models for physiological traits. To this end, we classified each dataset as

originating from a) a physiological, b) an emergent, or c) an interaction trait. Physiological traits directly depend on a small set of biochemical pathways and can be measured as fluxes or rates (e.g., gross photosynthesis rate, aerobic respiration rate). Emergent traits are the ultimate outcome of a wide diversity of cellular biochemical pathways and processes, and are not governed by species interactions. For example, the population growth rate of a sexually reproducing species depends on development rate, fecundity rate, and mortality rate, each of which is in turn dependent on a distinct set of biochemical processes that may also vary by life stage. Lastly, traits that explicitly describe species interactions were classified as interaction traits (e.g., resource consumption rate, filtration rate). We then extracted and compared the ten best-performing models across these three groups.

For physiological traits, none of the ten best-fitting models was mechanistic (Fig. 5A), whereas physiological, emergent, and interaction traits shared seven out of ten best-fitting models, albeit with different rankings (Fig. 5A-C and Supplementary Fig. 2). We reached similar conclusions after examining the ten best-fitting models for three vastly different traits with large numbers of thermal performance datasets across our data compilation: respiration rate (a physiological trait), population growth rate (an emergent trait), and resource consumption rate (an interaction trait). The three traits had six models in common among their ten best-fitting ones (Fig. 5D-F and Supplementary Fig. 3), whereas the interquartile ranges of AICc weights ranged from ≈ 0 to ~ 0.13. These results show that model performance is not strongly trait-dependent and that even when measurements come from traits that are governed by specific biochemical pathways, mechanistic models do not tend to outperform simpler phenomenological alternatives.

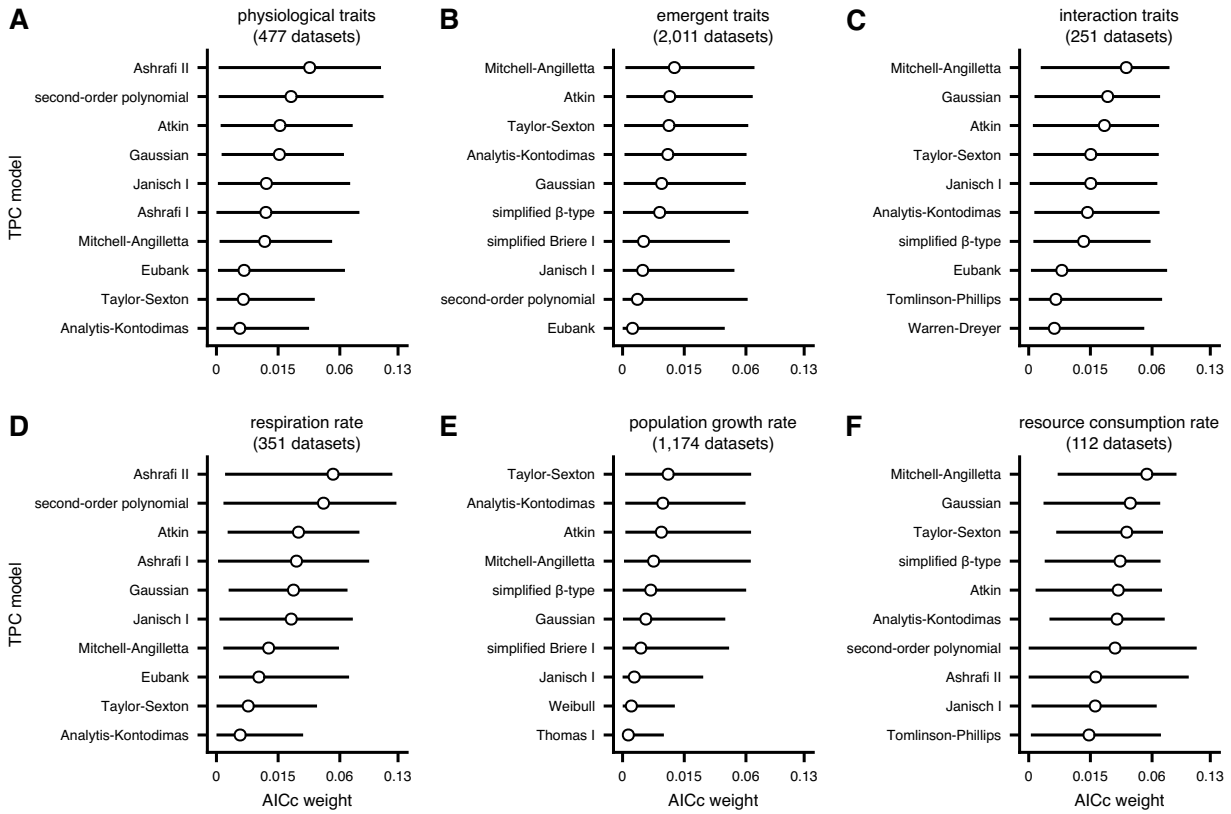

Fig. 5: The ten best-fitting models across thermal performance datasets from the three main trait groups (A-C) and for one representative trait per group (D-F). Circles represent the median AICc weight, whereas horizontal bars stand for the interquartile range. Similarly to Fig. 4, model performance varies predominantly within traits and to a much lesser extent among them (see also Supplementary Figs. 2 and 3). No model is able to consistently achieve high performance, even across different datasets of the same trait. Note that values along the horizontal axes do not increase linearly.

Predicting the optimal TPC model

Finally, we employed machine learning to uncover any rules for selecting the optimal TPC model(s) for a given thermal performance dataset. For this, we compiled 29 variables that describe the data in our study in four main aspects: i) the type of trait measured, ii) taxonomic information about the organism (kingdom and phylum), iii) the shape of the TPC

(e.g., its degree of skewness), and iv) sampling intensity (e.g., the number of distinct temperatures). The full list of variables along with their descriptions is available in Supplementary section S3. We then split the data into training and testing subsets (80% and 20% of the data, respectively) and fitted multi-output conditional inference regression trees[67] with different combinations of predictors using the R package `partykit`[68] (v. 1.2-17). This method aims at predicting multiple response variables simultaneously (here, the AICc weights of all models) based on binary splits using the values of predictor variables, selected through non-parametric tests. It ultimately yields data subsets (leaf nodes) that differ considerably in the composition of AICc weights, with the maximum number of such subsets being equal to two raised to the depth of the tree. For practical purposes, we set the maximum tree depth to four, allowing the algorithm to generate predictive rules for up to 16 different groups of thermal performance datasets. We also grouped rare levels of categorical predictors (those with fewer than 10 datasets) as 'other' to facilitate training. We determined the best-performing tree based on the R^2 value achieved on the training set, and also evaluated its performance across the separate testing subset.

Obtaining an accurate tree proved impossible as the best-fitting tree (Supplementary Fig. 4) had R^2 values of only 0.12 and 0.1 on the training and testing data subsets, respectively (Fig. 6A-B). More worryingly, the maximum predicted AICc weight by the tree was not greater than 0.22 (Fig. 6B). When we examined how accurately the tree predicted the AICc weights separately for each model, we found that the tree achieved its highest R^2 values (below 0.19) for models with a median AICc weight of ≈ 0 (Fig. 6C). In other words, the tree was slightly better able to predict the models that generally do not represent experimental data well, rather than the models that often provide good fits. Increasing the maximum tree depth to e.g., 10 (which would raise the number of leaf nodes to 1,024) or developing a more advanced predictive method based on deep learning could possibly yield more accurate predictions, but at a cost of limited interpretability.

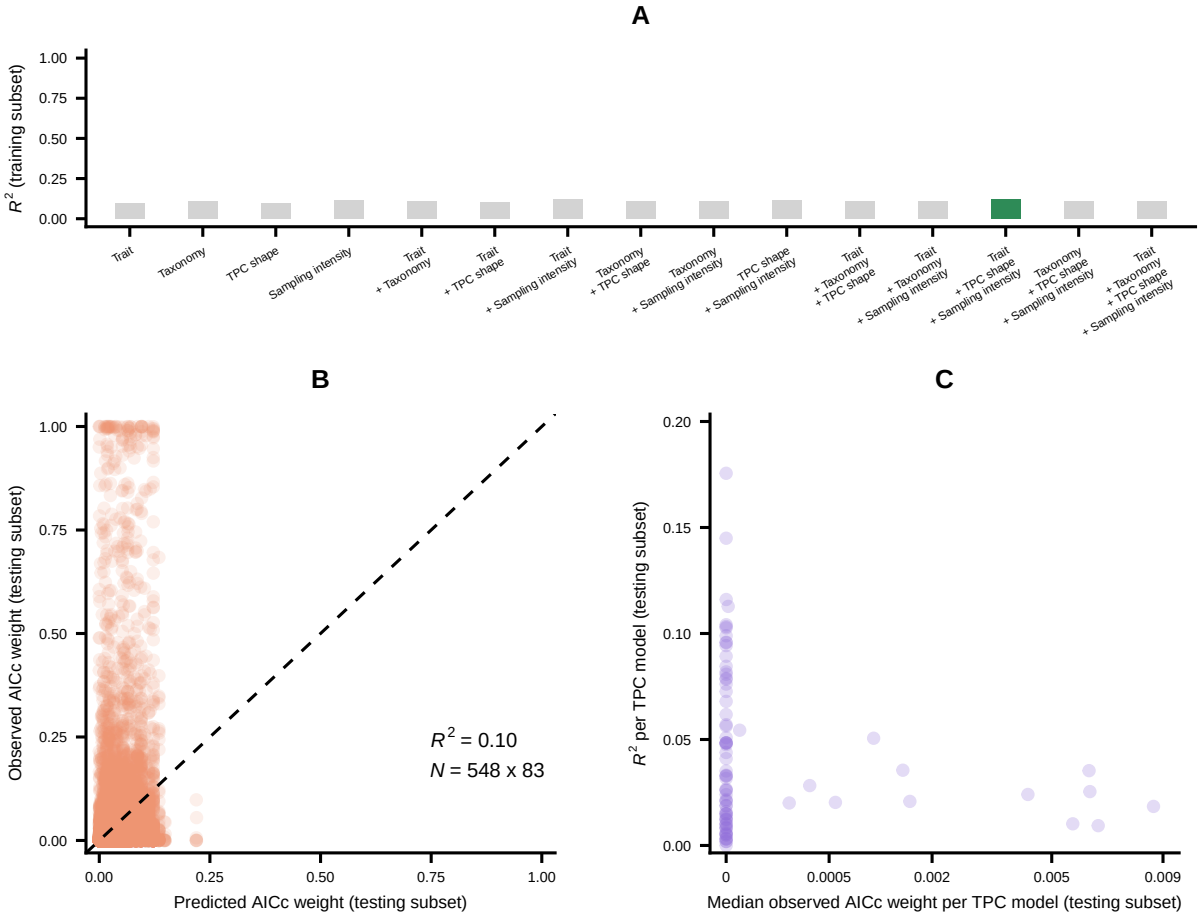

Fig. 6: Conditional inference trees with a maximum depth of four cannot accurately predict the AICc weights of TPC models. Panel A shows the R^2 values reached by alternative candidate trees (with different sets of predictor variables) across the subset of the data on which they were trained. The tree with the highest R^2 is highlighted in green. Panel B shows the predictions of the best tree (see Supplementary Fig. 4) versus the observed AICc weights across the testing subset (AICc weights of 83 models for 548 thermal performance datasets). The dashed line is the one-to-one line. Panel C shows the model-specific R^2 values achieved by the tree across the testing subset against the median observed AICc weight of each model.

Recommendations and conclusions

All our results converge on the same conclusion, i.e., that there are no simple and well-defined scenarios in which particular TPC models would be consistently favoured over others. This highlights the importance of performing model selection for objectively characterising the shape of thermal performance curves, instead of selecting a model in an arbitrary manner. Here, an anticipated objection might be that researchers often choose a particular model because it includes a parameter of interest for their study (e.g., $T_{\min}$, the temperature below which trait values become zero or negative; Fig. 1A). In such cases, our view is that model selection should still be considered, as multiple models may share the same parameter. Even when a model does not include the parameter of interest, it may be possible to obtain its value (either analytically or numerically) based on other model parameters or from the fitted curve itself.

We should clarify that we do not expect (or even recommend) ecophysiologists to fit all 83 models to each new thermal performance dataset. Instead, one could examine the dendrogram that we estimated in the present study (Fig. 3) to choose a subset of sufficiently distinct models (i.e., those branching far from each other) for fitting to a dataset. By using our dendrogram as a guide, researchers no longer need to compare the equations of different models manually, which can often be quite challenging in our experience. For example, our dendrogram shows that the Johnson-Lewin model[30] and a common modification thereof (the simplified Johnson-Lewin model; see Supplementary section S5) yield effectively identical fits, consistent with the conclusions of Yin and co-workers[69]. It is also worth pointing out that the fits of the mechanistic Johnson-Lewin model (and its variants) are typically highly similar to the fits of the phenomenological asymmetric Janisch model (Janisch II; Fig. 3), one of the two earliest-developed TPC models.

In conclusion, our study shows that for describing the shape of thermal performance curves, there is no "model to rule them all". Instead, ecophysiologists should adopt multi-

model approaches, identifying the most appropriate model(s) for a given dataset and research question. Such a strategy is likely to yield multiple benefits, such as bridging thermal biology "silos" (e.g., plant physiologists versus environmental microbiologists), improving study rigour and reproducibility, and ultimately enabling us to address increasingly challenging questions on the effects of temperature on biological systems.

Methods

Fitting TPC models to thermal performance datasets

Given that many of the models in our catalogue could not support non-positive trait measurements (e.g. negative population growth rate), we first removed such values from the datasets. To reduce the possibility of model overfitting, we only fitted a model to a thermal performance dataset if the parameters of the model were fewer than the number of distinct experimental temperatures. For fitting the models separately to each dataset, we used the R package `nls.multstart`[70,71] (v. 1.2.0). To find the optimal combination of parameter values that maximises the fit of a given TPC model to a given dataset, `nls.multstart` repeatedly fits the model using the Levenberg-Marquardt algorithm from different starting values. We specified seemingly realistic starting values for each model in various ways, depending on its parameters. For example, for models that include the $T_{\min}$ and $T_{\max}$ parameters (see Fig. 1), we set their starting values to the minimum and maximum experimental temperatures in the dataset, respectively. In some cases, we specified starting values by performing linear regression on a subset of the dataset (e.g., to estimate the slope of the rising part of the TPC) or by using parameter estimates from the literature. We then fitted each model to each thermal performance dataset 1,000 times. In every iteration, we used a different starting value per parameter, sampling from a uniform distribution with bounds equal to 0.5 and 1.5 times our initial starting value. To further facilitate the overall process, we fitted models to trait measurements on the natural logarithm scale, increased

the stringency of the convergence criteria by modifying the Levenberg-Marquardt parameters `ftol`, `ptol`, `maxiter`, and `maxfev`, set appropriate bounds for each TPC parameter where possible, and applied other checks (e.g., we forced T_{pk} to be $> T_{\mathrm{min}}$ and $< T_{\mathrm{max}}$). The source code for fitting the models is available from GitHub (`https://github.com/dgkontopoulos/Kontopoulos_et_al_83_TPC_models_2023`) and also archived on Zenodo (`https://doi.org/10.5281/zenodo.8328804`).

We calculated the AICc values of all model fits with an R^2 of at least 0.5. In a limited number of thermal performance datasets, the AICc value of at least one model was equal to $-\infty$, which is indicative of severe overfitting. When this was the case, we progressively removed the most parameter-rich models and examined the AICc values for that dataset again. If we still obtained values of $-\infty$ even when only three-parameter models were included, we excluded the corresponding dataset from our analyses. After this process, we ended up with 2,739 datasets out of the initial 3,598. We next constructed a table of AICc weights per model and per dataset. If a model could not converge on a specific dataset or was excluded for any of the aforementioned reasons, we assigned an AICc weight of 0.

Inferring a dendrogram of TPC models

To systematically compare the models in our catalogue, we first generated the curve for each model fit with an R^2 value greater than or equal to 0.5, across the 2,739 thermal performance datasets. This was done from the minimum experimental temperature of each dataset to the maximum temperature, with a step size of 0.1°C. We then constructed a matrix of pairwise Euclidean distances among curves (and, hence, models) per dataset, based on all aforementioned temperatures. Given that datasets varied considerably in the magnitude of their trait values, we performed maximum normalization[72] (also known as "l-infinity normalization") to ensure that pairwise distances were comparable across datasets. More specifically, we corrected each dataset-specific distance matrix by dividing its values

by the maximum height of all corresponding curves. We summarised the resulting distance matrices into a single (average) matrix, by taking the median of each cell across all matrices where possible. Finally, based on the average matrix, we calculated a dendrogram of TPC models using hierarchical clustering with average linkage, i.e., with the UPGMA[73] algorithm that has also been used for distance-based phylogenetic tree inference. Models that were placed in close proximity to each other in the dendrogram would generally produce very similar fits.

Data availability

The thermal performance datasets included in this study are available from Figshare: `https://doi.org/10.6084/m9.figshare.24106161.v1`.

Code availability

The source code for the main analyses of this study is available at `https://github.com/dgkontopoulos/Kontopoulos_et_al_83_TPC_models_2023` and archived at `https://doi.org/10.5281/zenodo.8328804`.

References

1. Angilletta, M. J. *Thermal adaptation: a theoretical and empirical synthesis* (Oxford University Press, 2009).

2. Clarke, A. *Principles of Thermal Ecology: Temperature, Energy, and Life* (Oxford University Press, 2017).

3. Chang, R. L. *et al.* Structural systems biology evaluation of metabolic thermotolerance in *Escherichia coli*. *Science* **340**, 1220–1223 (2013).

4. Chen, K. *et al.* Thermosensitivity of growth is determined by chaperone-mediated proteome reallocation. *Proc. Natl. Acad. Sci. U.S.A.* **114**, 11548–11553 (2017).

5. Li, G. *et al.* Bayesian genome scale modelling identifies thermal determinants of yeast metabolism. *Nat. Commun.* **12**, 190 (2021).

6. Higgins, J. K., MacLean, H. J., Buckley, L. B. & Kingsolver, J. G. Growth, developmental and stress responses of larvae of the clouded sulphur butterfly *Colias eriphyle* to repeated exposure to high, sub-lethal temperatures. *Physiol. Entomol.* **40**, 189–195 (2015).

7. Laurel, B. J., Copeman, L. A., Spencer, M. & Iseri, P. Temperature-dependent growth as a function of size and age in juvenile Arctic cod (*Boreogadus saida*). *ICES J. Mar. Sci.* **74**, 1614–1621 (2017).

8. Rollinson, N. *et al.* A new method of estimating thermal performance of embryonic development rate yields accurate prediction of embryonic age in wild reptile nests. *J. Therm. Biol.* **74**, 187–194 (2018).

9. Kontopoulos, D., Smith, T. P., Barraclough, T. G. & Pawar, S. Adaptive evolution shapes the present-day distribution of the thermal sensitivity of population growth rate. *PLoS Biol.* **18**, e3000894 (2020).

10. Cruz-Loya, M. *et al.* Antibiotics shift the temperature response curve of *Escherichia coli* growth. *mSystems* **6**, e00228–21 (2021).

11. Huxley, P. J., Murray, K. A., Pawar, S. & Cator, L. J. Competition and resource depletion shape the thermal response of population fitness in *Aedes aegypti*. *Commun. Biol.* **5**, 66 (2022).

12. Flanagan, P. H., Jensen, O. P., Morley, J. W. & Pinsky, M. L. Response of marine communities to local temperature changes. *Ecography* **42**, 214–224 (2019).

13. Gerhard, M., Koussoroplis, A. M., Hillebrand, H. & Striebel, M. Phytoplankton community responses to temperature fluctuations under different nutrient concentrations and stoichiometry. *Ecology* **100**, e02834 (2019).

14. Wieczynski, D. J. *et al.* Linking species traits and demography to explain complex temperature responses across levels of organization. *Proc. Natl. Acad. Sci. U.S.A.* **118**, e2104863118 (2021).

15. Yvon-Durocher, G. *et al.* Reconciling the temperature dependence of respiration across timescales and ecosystem types. *Nature* **487**, 472–476 (2012).

16. Reyes, W. M. *et al.* Complex terrain influences ecosystem carbon responses to temperature and precipitation. *Global Biogeochem. Cycles* **31**, 1306–1317 (2017).

17. Parain, E. C., Rohr, R. P., Gray, S. M. & Bersier, L.-F. Increased temperature disrupts the biodiversity–ecosystem functioning relationship. *Am. Nat.* **193**, 227–239 (2019).

18. Shocket, M. S. *et al.* Transmission of West Nile and five other temperate mosquito-borne viruses peaks at temperatures between 23°C and 26°C. *eLife* **9**, e58511 (2020).

19. Nguyen, K. H. *et al.* Interventions can shift the thermal optimum for parasitic disease transmission. *Proc. Natl. Acad. Sci. U.S.A.* **118**, e2017537118 (2021).

20. Kunze, C., Luijckx, P., Jackson, A. L. & Donohue, I. Alternate patterns of temperature variation bring about very different disease outcomes at different mean temperatures. *eLife* **11**, e72861 (2022).

21. Dell, A. I., Pawar, S. & Savage, V. M. Temperature dependence of trophic interactions are driven by asymmetry of species responses and foraging strategy. *J. Anim. Ecol.* **83**, 70–84 (2014).

22. García, F. C., Bestion, E., Warfield, R. & Yvon-Durocher, G. Changes in temperature alter the relationship between biodiversity and ecosystem functioning. *Proc. Natl. Acad. Sci. U.S.A.* **115**, 10989–10994 (2018).

23. Amarasekare, P. Effects of climate warming on consumer-resource interactions: a latitudinal perspective. *Front. Ecol. Evol.* **7**, 146 (2019).

24. Wagner, T. *et al.* Predicting climate change impacts on poikilotherms using physiologically guided species abundance models. *Proc. Natl. Acad. Sci. U.S.A.* **120**, e2214199120 (2023).

25. Kontopoulos, D.-G., García-Carreras, B., Sal, S., Smith, T. P. & Pawar, S. Use and misuse of temperature normalisation in meta-analyses of thermal responses of biological traits. *PeerJ* **6**, e4363 (2018).

26. Regehr, D. L. & Bazzaz, F. A. Low temperature photosynthesis in successional winter annuals. *Ecology* **57**, 1297–1303 (1976).

27. Janisch, E. Über die Temperaturabhängigkeit biologischer Vorgänge und ihre kurvenmäßige Analyse. *Pflüger's Arch. Physiol.* **209**, 414–436 (1925).

28. Angilletta Jr, M. J. Estimating and comparing thermal performance curves. *J. Therm. Biol.* **31**, 541–545 (2006).

29. Woods, H. A., Kingsolver, J. G., Fey, S. B. & Vasseur, D. A. Uncertainty in geographical estimates of performance and fitness. *Methods Ecol. Evol.* **9**, 1996–2008 (2018).

30. Johnson, F. H. & Lewin, I. The growth rate of *E. coli* in relation to temperature, quinine and coenzyme. *J. Cell. Comp. Physiol.* **28**, 47–75 (1946).

31. Ratkowsky, D. A., Olley, J. & Ross, T. Unifying temperature effects on the growth rate of bacteria and the stability of globular proteins. *J. Theor. Biol.* **233**, 351–362 (2005).

32. Hobbs, J. K. *et al.* Change in heat capacity for enzyme catalysis determines temperature dependence of enzyme catalyzed rates. *ACS Chem. Biol.* **8**, 2388–2393 (2013).

33. DeLong, J. P. *et al.* The combined effects of reactant kinetics and enzyme stability explain the temperature dependence of metabolic rates. *Ecol. Evol.* **7**, 3940–3950 (2017).

34. Ritchie, M. E. Reaction and diffusion thermodynamics explain optimal temperatures of biochemical reactions. *Sci. Rep.* **8**, 1–10 (2018).

35. Logan, J. A., Wollkind, D. J., Hoyt, S. C. & Tanigoshi, L. K. An analytic model for description of temperature dependent rate phenomena in arthropods. *Environ. Entomol.* **5**, 1133–1140 (1976).

36. Lactin, D. J., Holliday, N. J., Johnson, D. L. & Craigen, R. Improved rate model of temperature-dependent development by arthropods. *Environ. Entomol.* **24**, 68–75 (1995).

37. Briere, J.-F., Pracros, P., Le Roux, A.-Y. & Pierre, J.-S. A novel rate model of temperature-dependent development for arthropods. *Environ. Entomol.* **28**, 22–29 (1999).

38. Brown, J. H., Gillooly, J. F., Allen, A. P., Savage, V. M. & West, G. B. Toward a metabolic theory of ecology. *Ecology* **85**, 1771–1789 (2004).

39. Pawar, S., Dell, A. I. & Savage, V. M. From metabolic constraints on individuals to the dynamics of ecosystems. In *Aquatic functional biodiversity*, 3–36 (Elsevier, 2015).

40. Schoolfield, R. M., Sharpe, P. J. H. & Magnuson, C. E. Non-linear regression of biological temperature-dependent rate models based on absolute reaction-rate theory. *J. Theor. Biol.* **88**, 719–731 (1981).

41. Pawar, S., Dell, A. I., Savage, V. M. & Knies, J. L. Real versus artificial variation in the thermal sensitivity of biological traits. *Am. Nat.* **187**, E41–E52 (2016).

42. Molnár, P. K., Sckrabulis, J. P., Altman, K. A. & Raffel, T. R. Thermal performance curves and the metabolic theory of ecology—a practical guide to models and experiments for parasitologists. *J. Parasitol.* **103**, 423–439 (2017).

43. Dell, A. I., Pawar, S. & Savage, V. M. Systematic variation in the temperature dependence of physiological and ecological traits. *Proc. Natl. Acad. Sci. U.S.A.* **108**, 10591–10596 (2011).

44. Shi, P. & Ge, F. A comparison of different thermal performance functions describing temperature-dependent development rates. *J. Therm. Biol.* **35**, 225–231 (2010).

45. Krenek, S., Berendonk, T. U. & Petzoldt, T. Thermal performance curves of *Paramecium caudatum*: a model selection approach. *Eur. J. Protistol.* **47**, 124–137 (2011).

46. Shi, P.-J., Reddy, G. V., Chen, L. & Ge, F. Comparison of thermal performance equations in describing temperature-dependent developmental rates of insects: (I) empirical models. *Ann. Entomol. Soc. Am.* **109**, 211–215 (2016).

47. Shi, P.-J., Reddy, G. V., Chen, L. & Ge, F. Comparison of thermal performance equations in describing temperature-dependent developmental rates of insects: (II) two thermodynamic models. *Ann. Entomol. Soc. Am.* **110**, 113–120 (2017).

48. Low-Décarie, E. *et al.* Predictions of response to temperature are contingent on model choice and data quality. *Ecol. Evol.* **7**, 10467–10481 (2017).

49. Quinn, B. K. Performance of the SSI development function compared with 33 other functions applied to 79 arthropod species' datasets. *J. Therm. Biol.* **102**, 103112 (2021).

50. Corkrey, R., Olley, J., Ratkowsky, D., McMeekin, T. & Ross, T. Universality of thermodynamic constants governing biological growth rates. *PLoS One* **7**, e32003 (2012).

51. Amarasekare, P. & Savage, V. A framework for elucidating the temperature dependence of fitness. *Am. Nat.* **179**, 178–191 (2012).

52. Smith, T. P. *et al.* Community-level respiration of prokaryotic microbes may rise with global warming. *Nat. Commun.* **10**, 1–11 (2019).

53. Kontopoulos, D.-G. *et al.* Phytoplankton thermal responses adapt in the absence of hard thermodynamic constraints. *Evolution* **74**, 775–790 (2020).

54. García-Carreras, B. *et al.* Role of carbon allocation efficiency in the temperature dependence of autotroph growth rates. *Proc. Natl. Acad. Sci. U.S.A.* **115**, E7361–E7368 (2018).

55. Ikeda, T. Marine zooplankton metabolic data ver. 2. http://hdl.handle.net/2115/76282 (2019).

56. Acuña, J. L., López-Urrutia, Á. & Colin, S. Faking giants: the evolution of high prey clearance rates in jellyfishes. *Science* **333**, 1627–1629 (2011).

57. López-Urrutia, Á., San Martin, E., Harris, R. P. & Irigoien, X. Scaling the metabolic balance of the oceans. *Proc. Natl. Acad. Sci. U.S.A.* **103**, 8739–8744 (2006).

58. DeLong, J. *et al.* Habitat, latitude and body mass influence the temperature dependence of metabolic rate. *Biol. Lett.* **14**, 20180442 (2018).

59. Nilsson-Örtman, V., Stoks, R., De Block, M., Johansson, H. & Johansson, F. Latitudinally structured variation in the temperature dependence of damselfly growth rates. *Ecol. Lett.* **16**, 64–71 (2013).

60. Phillips, J. A. *et al.* The effects of phylogeny, habitat and host characteristics on the thermal sensitivity of helminth development. *Proc. R. Soc. Lond. B Biol. Sci.* **289**, 20211878 (2022).

61. Lear, K. O. *et al.* Thermal performance responses in free-ranging elasmobranchs depend on habitat use and body size. *Oecologia* **191**, 829–842 (2019).

62. Dell, A. I., Pawar, S. & Savage, V. M. The thermal dependence of biological traits. *Ecology* **94**, 1205–1206 (2013).

63. Ruggiero, M. A. *et al.* A higher level classification of all living organisms. *PLoS ONE* **10**, e0119248 (2015).

64. Sugiura, N. Further analysis of the data by Akaike's information criterion and the finite corrections. *Commun. Stat. Theory Methods* **7**, 13–26 (1978).

65. Yu, G., Smith, D. K., Zhu, H., Guan, Y. & Lam, T. T.-Y. ggtree: an R package for visualization and annotation of phylogenetic trees with their covariates and other associated data. *Methods Ecol. Evol.* **8**, 28–36 (2017).

66. Gu, Z. Complex heatmap visualization. *iMeta* **1**, e43 (2022).

67. Hothorn, T., Hornik, K. & Zeileis, A. Unbiased recursive partitioning: A conditional inference framework. *J. Comput. Graph. Stat.* **15**, 651–674 (2006).

68. Hothorn, T. & Zeileis, A. partykit: A modular toolkit for recursive partytioning in R. *J. Mach. Learn. Res.* **16**, 3905–3909 (2015).

69. Yin, X. No need to switch the modified Arrhenius function back to the old form. *New Phytol.* **231**, 2113–2116 (2021).

70. Padfield, D. & Matheson, G. *nls.multstart: Robust Non-Linear Regression using AIC Scores* (2020). URL `https://CRAN.R-project.org/package=nls.multstart`. R package version 1.2.0.

71. Padfield, D., O'Sullivan, H. & Pawar, S. *rTPC* and *nls.multstart*: A new pipeline to fit thermal performance curves in R. *Methods Ecol. Evol.* **12**, 1138–1143 (2021).

72. Quarteroni, A., Sacco, R. & Saleri, F. *Numerical Mathematics* (Springer, 2010).

73. Sokal, R. R. & Michener, C. D. A statistical method for evaluating systematic relationships. *University of Kansas Science Bulletin* **38**, 1409–1438 (1958).

Acknowledgements

AS was supported by the ANR project EcoTeBo (ANR-19-CE02-0001-01) from the French National Research Agency (ANR). We are grateful to Perng Lee, Olivia Morris, and Alejandro Isla for providing some of the thermal performance datasets used in this study.

Competing interests

The authors have no competing interests to declare.

Correspondence and requests for materials should be addressed to D.G.K.